

CFD Analysis of the Radial Blower Performance for Telecommunication System Cooling

Vankudoth Raju

*Dept. of Mechanical Engineering,
PCET Hyderabad*

Abstract: Computational fluid dynamics (CFD) model for fans and radial blowers involve about blades and geometry, flow angles, blades rotational speed, and flow velocities. Accurate simulations of such models require large number of mesh points which is beyond the allocated time and available resources for engineering design cycles. When dealing with system or broad level thermal analysis, where a fan or blower is among many components need to be modelled, a macro representation of a fan or a blower is preferred. A macro model of a fan is a plane surface that includes pressure across as the flow passes through it. The pressure airflow relationship is taken from the fan curve provided by the fan made manufacture. A macro model for a radial blower is more involved because of the 90 degree flow turn inside the blowers housing and induced flow swirl caused by impeller blades. The need to capture the flow turn and induced swirl becomes more pronounced when simulating multiple interacting blowers inside a blowers tray. In this paper, a systematic approach is presented to design the blower macro from the existing the fan model. the pack CFD results for the blower tray have been analyzed. A typical use of three fan blower tray in a system representing telecommunication application is also presented at the end.

Keywords: CFD, Flow Angles, Pressure, Blower.

Introduction

Axial flow fan is extensively used in many engineering applications. Its adaptability has resulted in implementation into large scale systems, from industrial dryers and air conditioning units to automotive engine cooling and in-cabin air recirculation systems. The benefit of using axial flow fans for the purpose of augmenting heat transfer is particularly evident in the automobile industry because of the need for relatively compact designs. The extended use of axial flow fans for fluid movement and heat transfer has resulted in detailed research into the performance attributes of many designs. Numerical investigations have been performed to quantify the performance of axial fans and their flow characteristics. However, the more-practical example of cooling a heated engine or heated plate using an axial flow fan has received more attention in regards to understanding flow characteristics and heat transfer. With the expressive computer capability and extensive development in the simulation field, CFD have drawn attention in recent years.

An internal combustion engine (ICE) is a heat engine where the combustion of a fuel occurs with an oxidizer (usually air) in a combustion chamber that is an integral part of the working fluid flow circuit. In an internal combustion engine the expansion of the high-temperature and high-pressure gases produced by combustion apply direct force to some component of the engine. The force is applied typically to pistons, turbine blades, or a nozzle. This force moves the component over a distance, transforming chemical energy into useful mechanical energy. Internal combustion engine cooling uses either air or a liquid to remove the waste heat from an internal combustion engine. For small or special purpose engines, air cooling makes for a lightweight and relatively simple system. The more complex circulating liquid-cooled engines also ultimately reject waste heat to the air, but circulating liquid improves heat transfer from internal parts of the engine. Engines for watercraft may use open-loop cooling, but air and surface vehicles must recalculate a fixed volume of liquid. Radiators are heat exchangers used for cooling internal combustion engines, mainly in automobiles but also in piston-engine aircraft, railway locomotives, motorcycles, stationary generating plant or any similar use of such an engine. Internal combustion engines are often cooled by circulating a liquid coolant through the engine block, where it is heated and through a radiator where it loses heat to the atmosphere, and then returned to the engine. Engine coolant is usually water-based, but may also be oil. It is common to employ a water pump to force the engine coolant to circulate, and also for an axial fan to force air through the radiator. A cooling system works by sending a liquid through passage in the engine block and heads. As the coolants flow through this passage it picks up the heat from the engine. The heated liquid makes its way to the radiator through a rubber hose. This liquid is cooled by air stream entering the engine compartment from the grill in front of the car. A thermostat is placed between the engine and the radiator to make sure that the coolant stays above a certain

temperature. If the coolant temperature falls below this temperature, the thermostat blocks the coolant flow to the radiator, forcing the fluid instead through a bypass directly back to the engine. In order to prevent the coolant from boiling, the cooling system is designed to be pressurized. Under the pressure the boiling point of the coolant is raised considerably. However too much pressure will result to burst of hoses, so system is needed to relieve pressure if it exceeds a certain point, this work is done by radiator cap.

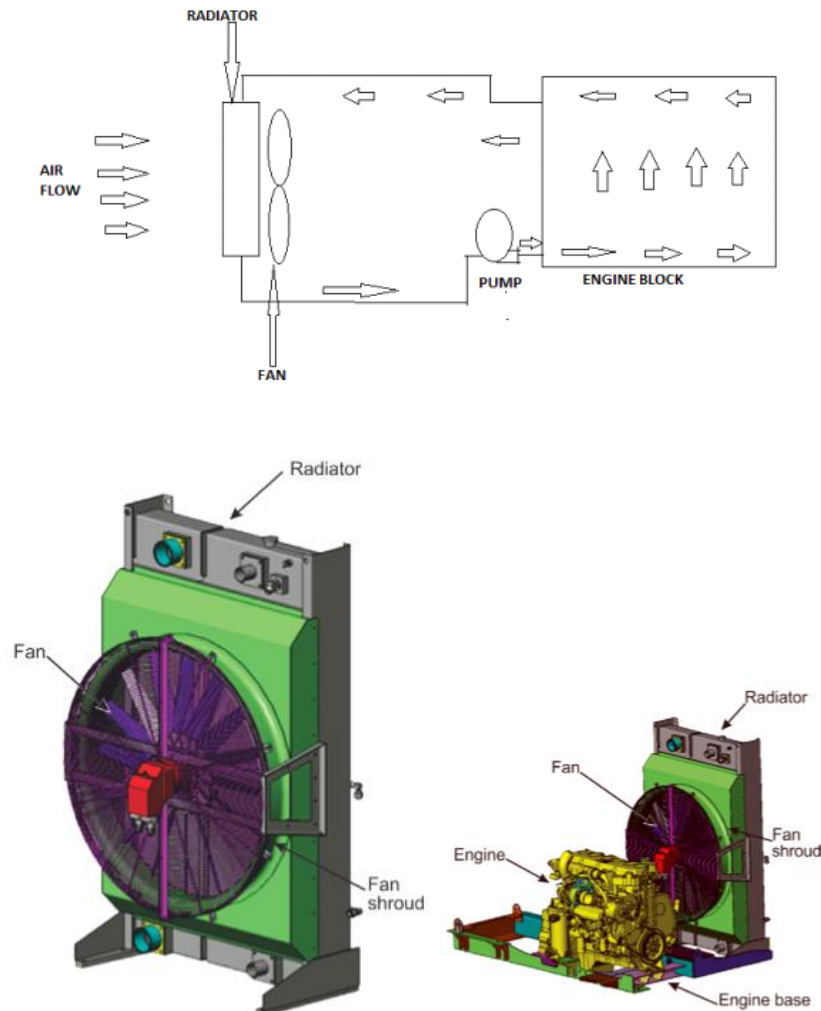


Fig. 1 Radiator fan assembly & Cooling System

1.2 Objective

The efficiency of automotive radiator is largely dependent on the ability of the fan to force the air draught as much as possible. In order to devise an effective fan design, the primary objective is to maintain desired pressure difference between the fan inlet and outlet.

The radiator fan design was first evaluated through simulations to obtain pressure difference and torque values. In order to obtain the desired pressure difference and torque.

The radiator fan with 12 blades was first analyzed through CFD simulations and the pressure difference between the fan inlet and outlet were measured. To improve performance keeping the same number of blade and discharge with changing the rotational speed of the fan were suggested and flow analysis for the same was performed. Desired pressure difference was obtained through the various rotational speeds. Final results show better efficiency calculating by the numerical simulation. This solution can also be provided using FLUENT.

Literature Survey

Priti Pramod Bodkhe and JP Yadav¹, Mechanical Department MITCOE Pune in their studies, also presented parametric study on automotive radiator. In the performance study evaluation, radiator is installed into a setup. The various parameters including mass flow rate of cooling, inlet coolant temperature, etc are varied. Dittus, W., & Boelter², Pioneers in Heat Transfer in Automobile Radiator of Tubular type the conclusion of their studies shows the heat transfer increases with nanoparticles volume concentration in the subchannel geometry. The highest heat transfer rates are detected, for each concentration, corresponding to the higher Reynolds number. John R Howell³, The History of Engineering Radiation in Heat Transfer his research has centered on developing solution techniques for radiative transfer in participating media, solution of highly non-linear combined mode heat transfer problems and most recently inverse design and control of thermal system with combined mode (non-linear) heat transfer. Ying Gaun, Hongjiang Cui, Minghai Li⁴ Carried work on engine cooling system with heat load averaging capacity using passive heat load accumulator. Heat load accumulator is phase change material which stores heat generated during peak and dissipates stored heat during reduced heat load condition. This is achieved by sacrificing phase change of PCM from solid to liquid or vice versa. This leads to compact heat exchanger for same heat rejection. Also it reduces load on cooling system. Dzyubenko, B.V., Drester⁵, G.A., D.M. Dawson discussed about hydraulic actuated cooling system. Actuators can improve temperature tracking and reduce parasitic losses. Actuator based engine cooling system uses controller to control coolant pump and radiator fan operating conditions. It provides power to system component as per requirement. Thus it regulates power consumption of system component with cooling capacity. A non-linear back stepping robust controller is used to regulate engine coolant temperature in hydraulic based thermal management system. K.Y. Leong⁶, R. Saidur, S.N. Kazi, A.H. Mamun⁷ described use of nanofluid based coolant in engine cooling system and its effect on cooling capacity. It is found that 565 nanofluid having higher thermal conductivity than base coolant like 50%/50% water and ethylene glycol. It increases heat transfer. Y Hirayana⁸ explained conventional radiator size is rectangular which is difficult for circular fan to cover whole surface area. It creates lower velocity zone at corners giving less heat transfer. Author has proposed to eliminate corners and develop circular shape radiator which is compact, more efficient and leads to minimum power consumption to drive fan and maximum utilization of air flow.

Hwa-Ming Nieh, Tun-Ping Teng, Chao-Chieh Yu [2], and This study adopt an alumina (Al₂O₃) and titanium (TiO₂) Nano-coolant to enhance the heat dissipation performance of an air-cooled radiator. The two-step synthesis method is used to produce different concentrations of Al₂O₃ and TiO₂/water (W) Nano fluid by using a 0.2 wt. % chitosan dispersant, and the Nano fluid is mixed with ethylene glycol (EG) at a 1:1 volume ratio to form NC1 to NC6 (Nano Coolant). The experiments were conducted to measure the thermal conductivity, viscosity, and specific heat of the NC with different concentrations of nanoparticles and sample temperatures, and then the NC was used in an air-cooled radiator to evaluate its heat dissipation capacity, pressure drop, and pumping power under different volumetric flow rates and heating temperatures. The experimental results show that the heat dissipation capacity and the EF of NC are higher than EG/W, and that the TiO₂ NC are higher than Al₂O₃ NC in most of the experimental data. The enhanced percentage of the average EF increases as the concentration and volumetric flow rate of the TiO₂ NC increases. M. Naraki and S.M. Peyghambarzadeh [3], In this research, the overall heat transfer coefficient of CuO/water Nano fluids is investigated experimentally under laminar flow regime (100 < Re < 1000) in a car radiator. The Nano fluids in all the experiments have been stabilized with variation of pH and use of suitable surfactant. The results show that the overall heat transfer coefficient with Nano fluid is more than the base fluid. The overall heat transfer coefficient increases with the enhancement in the Nano fluid concentration from 0 to 0.4 vol. %. Conversely, the overall heat transfer coefficient decreases with increasing the Nano fluid inlet temperature from 50 to 80 °C.

In this article, the experimental overall heat transfer coefficient in the automobile radiator has been measured using CuO/water Nano fluid at different air and liquid volumetric flow rates, various Nano fluid concentrations and several inlet temperatures of the liquid. Also, the results have been statistically analyzed using Taguchi method. Rahul Tarodiya, J. Sarkar, J. V. Tirkey [4], the use of "Nano fluids" have been developed and these fluids offer higher heat transfer properties compared to that of conventional automotive engine coolants. Energetic analyses as well as theoretical performance analyses of the flat fin tube automotive radiator using Nano fluids as coolants have been done to study its performance improvement. Effects of various operating parameters using Cu, SiC, and Al₂O₃ and TiO₂ Nano fluids with 80% water- 20% ethylene glycol as a base fluid are presented in this article. Use of Nano fluid as coolant in radiator improves the effectiveness, cooling capacity with the reduction in pumping power. SiC-80% H₂O-20% EG (base fluid) yields best performance in radiator having plate fin geometry followed by Al₂O₃-base fluid, TiO₂-base fluid and Cu-base fluid. The maximum cooling improvement for SiC is 18.36%, whereas that for Al₂O₃ is 17.39%, for TiO₂ is 17.05% and for Cu is 13.41% as coolants. Present study reveals that the Nano fluids may effectively use as

coolant in automotive radiators to improve the performance. Efeovbokhan, Vincent Enontiemonria, Ohiozua, OhiremeNathaniel [5], The cooling properties of a locally formulated coolant (sample C) vis-a-vis, its boiling characteristics and specific heat capacity were investigated alongside with a common coolant-water (as sample A) and a commercial coolant (sample B). The results of the investigation showed that sample C gave the best performance compared to the other two samples A and B: the boiling points of sample C was 1100C, sample A 1000C, and sample B 1010C. This means that the possibility of a boil-out of sample C from the radiator is little compared to samples A and B. Also, for the same quantity of coolant more heat would be required to raise sample C to its boiling point than for samples A and B. In other word, better cooling would be achieved using sample C. S.M. Peyghambarzadeh, S.H. Hashemabadi, S.M. Hoseini, M. Seifi Jamnani [6], Traditionally forced convection heat transfer in a car radiator is performed to cool circulating fluid which consisted of water or a mixture of water and anti-freezing materials like ethylene glycol (EG). In this paper the heat transfer performance of pure water and pure EG has been compared with their binary mixtures. Furthermore, different amounts of Al₂O₃ nanoparticle have been added into these base fluids and its effects on the heat transfer performance of the car radiator have been determined experimentally. Liquid flow rate has been changed in the range of 2–6 l per minute and the fluid inlet temperature has been changed for all the experiments. The results demonstrate that Nano fluids clearly enhance heat transfer compared to their own base fluid. In the best conditions, the heat transfer enhancement of about 40% compared to the base fluids has been recorded. S.M. Peyghambarzadeh, S.H. Hashemabadi, M. Naraki, Y. Vermahmoudi, [7], the heat transfer performance of the automobile radiator is evaluated experimentally by calculating the overall heat transfer coefficient (U) according to the conventional \square -NTU Technique. Copper oxide (CuO) and Iron oxide (Fe₂O₃) nanoparticles are added to the Water at three concentrations 0.15, 0.4, and 0.65 vol. % with considering the best pH for longer stability. In these experiments, the liquid side Reynolds number is varied in the range of 50-1000 and the inlet liquid to the radiator has a constant temperature which is changed at 50, 65 and 80 0C. The effects of these variables on the overall heat transfer coefficient are deeply investigated. Nano fluids showed greater heat transfer performance comparing with water. Increasing liquid and air Re increases the overall heat transfer coefficient. Increasing the inlet liquid temperature decreases the overall heat transfer coefficient. D. Madhesh, R. Parameshwaran, S. Kalaiselvam, [8] an investigate the heat transfer potential and rheological characteristics of copper–titania hybrid Nano fluids using a tube in the tube type counter flow heat exchanger. The Nano fluids were prepared by dispersing the surface functionalized and crystalline copper–titania hybrid Nano composite in the base fluid, with volume concentrations ranging from 0.1% to 2.0%. The surface functionalized and highly crystalline nature of hybrid nano composite have contributed to the creation of effective thermal interfaces with the fluid medium, thereby enabling the achievement of achieving improved thermal conductivity and heat transfer potential of Nano fluids. The effective thermal conductivity and diffusion kinetics of hybrid nano composite in the fluid medium paved the way for the improved heat transfer Characteristics of hybrid nano fluid. Navid Bozorgan, Komalangan Krishnakumar, Nariman Bozorgan [9], The heat transfer relations between airflow and Nano fluid coolant have been obtained to evaluate local convective and overall heat transfer coefficients and also pumping power for Nano fluid flowing in the radiator with a given heat exchange capacity. In the present study, the effects of the automotive speed and Reynolds number of the Nano fluid in the different volume concentrations on the radiator performance are also investigated. The overall heat transfer coefficient of Nano fluid is greater than that of water alone and therefore the total heat transfer area of the radiator can be reduced. However, the considerable increase in associated pumping power may impose some limitations on the efficient use of this type of Nano fluid in automotive diesel engine radiators. L. Syam Sundar, Manoj K. Singh, Igor Bidkin, Antonio C.M. Sousa [10], A magnetic Nano fluid was prepared by dispersing magnetic Ni nanoparticles in distilled water. The Nano-particles were synthesized by chemical coprecipitation method and characterized by X-ray diffraction and atomic force microscopy. The average particle size was measured by the dynamic light scattering method. Thermal conductivity and absolute viscosity of the Nano fluid were experimentally determined as a function of particle concentration and temperature. In addition, the Nusselt number and friction factor were experimentally estimated as a function of particle concentration and Reynolds number for constant heat flux condition in forced convection apparatus with no phase change of the Nano fluid flowing in a tube. The experiments were conducted for a Reynolds number range of 3000–22,000, and for a particle concentration range from 0% to 0.6%. The results indicate that both Nusselt number and friction factor of the Nano fluid increase with increasing particle volume concentration and Reynolds number. For 0.6% volume concentration, the enhancement of Nusselt number and friction factor is 39.18% and 19.12%, respectively, as compared to distilled water under the same flow conditions. It was verified the classical Gnielinski and Nottter–Rouse correlations under predict the Nusselt number of the Nano fluid; therefore, new generalized correlations are proposed for the estimation of the Nusselt number and friction factor based on the experimental data.

Changhua Lin, Jeffrey Saunders, Simon Watkins [11], A theoretical model for the calculation of Specific Dissipation (SD) was developed. Based on the model, the effect of ambient and coolant radiator inlet temperatures on SD has been predicted. Results indicate that the effect of A Review Paper on Analysis of Automobile Radiator (IJSRD/Vol. 2/Issue 08/2014/094) All rights reserved by www.ijsrd.com 413 ambient and coolant inlet temperature variation on SD is small (less than 2%) when ambient temperature varies between 10 and 50°C and coolant radiator inlet temperature between 60 and 120°C. The effect of coolant flow rate on SD is larger if there is a larger flow rate variation. Experimental results indicate that a 1 % variation at 1.0 L/s will cause about $\pm 0.6\%$ SD Variation. Therefore the flow rate should be carefully controlled. Shaolin Maoa, Changrui Cheng, Xianchang Li, Efstathios E. Michaelides [12], A thermal/structural coupling approach is applied to analyze thermal performance and predict the thermal stress of a radiator for heavy-duty transportation cooling systems. Bench test and field test data show that non-uniform temperature gradient and dynamic pressure loads may induce large thermal stress on the radiator. A finite element analysis (FEA) tool is used to predict the strains and displacement of radiator based on the solid wall temperature, wall-based fluid film heat transfer coefficient and pressure drop. These are obtained from a computational fluid dynamics (CFD) simulation. The FEA results predict the maximum value of stress/strain and target locations for possible structural failure and the results obtained are consistent with experimental observations. The results demonstrate that the coupling thermal/structural analysis is a powerful tool applied to heavy-duty cooling product design to improve the radiator thermal performance, durability and reliability under rigid working environment. M.M. Elias, I.M. Mahbubul, R. Saidur, M.R. Sohel, I.M. Shahrul, S.S. Khaleduzzaman, S. Sadeghipour [13], Nano fluid is a new type of heat transfer fluid with superior thermal performance characteristics, which is very promising for thermal engineering applications. This paper presents new findings on the thermal conductivity, viscosity, density, and specific heat of Al₂O₃ Nano particles dispersed into water and ethylene glycol based coolant used in car radiator. The Nano fluids were prepared by the two-step method by using an ultrasonic homogenizer with no surfactants. Thermal conductivity, viscosity, density, and specific heat have been measured at different volume concentrations (i.e. 0 to 1 vol. %) of nanoparticles and various temperature ranges (i.e. from 10 °C to 50 °C). It was found that thermal conductivity, viscosity, and density of the Nano fluid increased with the increase of volume concentrations. However, specific heat of Nano fluid was found to be decreased with the increase of nanoparticle volume concentrations. Moreover, by increasing the temperature, thermal conductivity and specific heat were observed to be intensified, while the viscosity and density were decreased. Adnan M. Hussein, R.A. Bakar, K. Kadirgama,

Introduction to Fluid Mechanics

3.1 Introduction:

Fluids are very familiar to us. Our body itself is mostly water while what surrounds us is largely air, which again is a fluid. In fact, Greeks and Indians in the past worshiped earth, fire, sky, water and air three of these being fluids. Fluid Mechanics is a science that studies the behavior of fluids and its effect on other bodies. It comprises of Fluid Statics, which is a study of fluids at rest and Fluid Dynamics, which is a study of fluid in motion.

There are three approaches to Fluid Mechanics – Experimental, Theoretical and Computational. Experimental approach is the oldest approach, perhaps also employed by Archimedes when he was to investigate a fraud. It is a very popular approach where you will make measurements using a wind tunnel or similar equipment. But this is a costly venture and is becoming costlier day by day. Then we have the theoretical approach where we employ the mathematical equations that govern the flow and try to capture the fluid behavior within a closed form solution i.e., formulas that can be readily used. This is perhaps the simplest of the approaches, but its scope is somewhat limited. Not every fluid flow renders itself to such an approach. The resulting equations may be too complicated to solve easily. Then comes the third approach- Computational. Here we try to solve the complicated governing equations by computing them using a computer. This has the advantage that a wide variety of fluid flows may be computed and that the cost of computing seems to be going down day by day. With the result the emerging discipline Computational Fluid Dynamics, CFD, has become a very powerful approach today in industry and research.

3.2 Fluid:

It is well known that matter is divided into solids and fluids. Fluids can be further divided into Liquids and Gases. Solids have a definite shape and a definite size, while the liquids have a definite size, but no definite shape. They assume the shape of the container they are poured into. Gases on the other hand have neither a shape nor a size. They can fill any container fully and assume its shape.

3.3 Methods to Study Fluid Flow:

3.3.1 Lagrangian Method:

In this a fluid particle is selected, which is pursued throughout its course of motion. And changes in its parameters are studied.

3.3.2 Eulerian Method:

In this method any point in the space occupied by the fluid is selected and observation is made on changes in fluid parameters at the point.

3.4 Different Types of Flows:

3.4.1 Compressible vs incompressible flow:

A fluid problem is called compressible if the pressure variation in the flow field is large enough to effect substantial changes in the density of the fluid. Flows of liquids with pressure variations much smaller than those required to cause phase change (cavitation), or flows of gases involving speeds much lower than the isentropic sound speed are termed incompressible

$$\text{Mach number} = \frac{\text{Mach number}}{\text{Mach number}} = \frac{\text{Incompressible flow}}{\text{Compressible flow}}$$

3.4.2 Steady vs unsteady flow:

Depending on the parameters on which fluid flow depends with respect to time, it is of classified two types, Steady & Unsteady. If fluid flow is dependent on time it is an Unsteady flow else if is independent of time it is a Steady flow. Both the Navier-Stokes equations and the Euler equations become simpler when their steady forms are used. Whether a problem is steady or unsteady depends on the frame of reference. For instance, the flow around a ship in a uniform channel is steady from the point of view of the passengers on the ship (the Lagrangian Reference Frame), but unsteady to an observer on the shore (the Eulerian Reference Frame). Fluid dynamics often transform problems to frames of reference in which the flow is steady in order to simplify the problem

$$k' = \frac{\text{Unsteady flow}}{\text{Steady flow}} \text{ Velocity, Pressure, Density, Temperature etc.,}$$

3.4.3 Uniform vs Non-uniform Flow:

If the fluid velocity does not change, both in magnitude & direction from point to point for any given instant of time, the flow is considered as uniform flow, else if the velocity changes with respect to displacement of fluid it is Non-uniform flow.

$$\frac{\text{Uniform flow}}{\text{Non-Uniform flow}}$$

3.4.4 Laminar vs Turbulent Flow:

If the fluid particles move in layers with one layer of fluid sliding smoothly over the adjacent layer, such that the paths of the individual fluid particles do not cross into the neighboring layers. Generally it occurs at low velocity so that forces due to viscosity predominate over the inertial forces. The viscosity of fluid induces relative motion within the fluid as the fluid layers slide over each other, which in turn give rise to shear stresses. The magnitude of viscous shear stress so produced, varies from point to point, being maximum at the boundary and gradually decreasing with increase in distance from the boundary.

A fluid motion is said to be turbulent when the fluid particles move in an entirely haphazard or disorderly manner that results in a rapid and continuous mixing of fluid leading to momentum transfer as fluid flows. So causes to formation of fluctuations in the velocity & pressure at any point in flow, which is a function of time.

$$\frac{\text{Relation between shear \& pressure gradients in laminar flow}}{\text{Total shear stress at any point in turbulent flow.}}$$

3.4.5 Rotational & Irrotational Flow:

A flow is said to be rotational if the fluid particles while moving along in the direction of flow rotate about their mass centers. The velocity of each particle varies directly as the distance from the center of rotation.

A flow is said to be irrotational if the fluid particles while moving in the direction of the flow do not rotate about their mass centers.

3.5 Models of the Flow:

In obtaining the basic equations of fluid motion, the following philosophy is always followed:

1. Choose the appropriate fundamental physical principles from the law of physics

Such as:

- a. Mass conserved
 - b. $F=ma$ (Newton second law)
 - c. energy conserved.
2. Apply these principles to a suitable model of the flow.
 3. From this application, extra the mathematical equations which embody such physical Principles.

A solid body is rather easy to see & define; on the other hand, a fluid is a “squishy” substance that is hard to grab hold of. If a solid body is in translation motion, the velocity of each part of the body is the same; on the other hand, if a fluid motion, the velocity may be different at each location in the fluid. How then do we visualize a moving fluid so as to apply to it the fundamental physical principles? For a continuum fluid the answer is to construct one of the 4 models described below.

3.5.1 Finite Control Volume

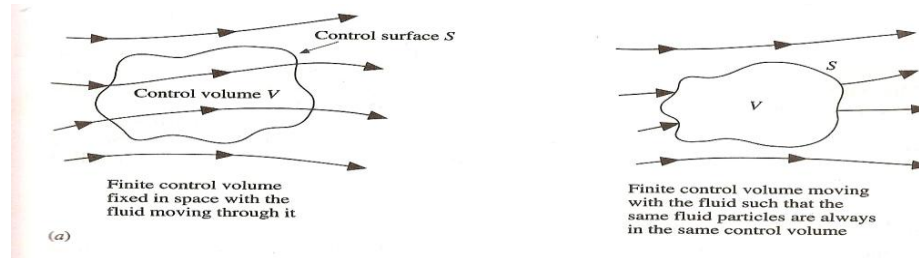


Fig 3.1: closed volume within the finite region of the flow

Consider a general flow field as represented by the streamlines in fig 3.1. Let us imagine a closed volume drawn within the finite region of the flow. This volume defines a control volume V ; a control surface S is defined as the closed surface which bounds the volume. The control volume may be fixed in space with in the fluid moving trough it, as shown at the left fig 3.1. Alternatively, the control volume moving with the fluid such that the same that the same fluid particles are always moving inside it, as shown at the right of fig3.1. In the either case, the control volume is a reasonable large, finite region of the flow. The fundamental physical principles are applied to the fluid inside the control volume & to the fluid crossing the control surface. Therefore, instead of looking at the whole flow field at once, with the control volume model we limit our attention to just the fluid in the finite region of the volume itself. The fluid flow equations that we directly obtain by applying the fundamental physical principles to a finite control volume are in integral form. These integral forms of the governing equations. Can be manipulated to indirectly obtain partial differential equations. These equations. So obtained from the finite control volume fixed in space (left side of fig.3.1), in either integral or partial differential form, are called the conservation form of the governing equations. The equations Obtained from the finite control volume moving with the fluid (right side of fig.3.1) in either integral or partial differential form are called then non-conservation form of the governing equations.

3.5.2 Infienitsimal Fluid Element:

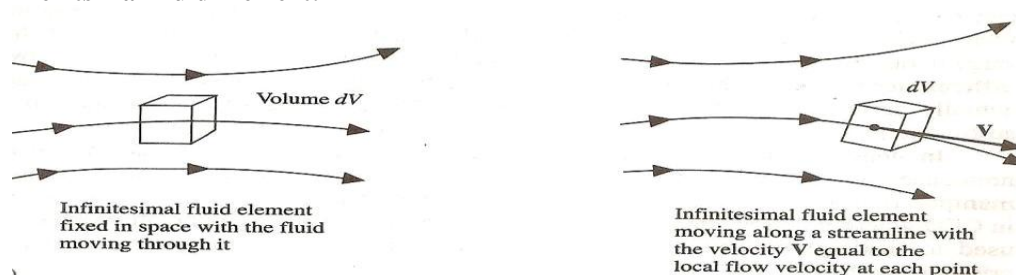


Fig 3.2: infinitesimally small fluid element in the flow with differential volume

Consider a general flow field as represented by stream lines in fig 3.2. Let us imagine an infinitesimally small fluid element in the flow with differential volume dv . The fluid element is infinitesimal in the same sense as differential calculus; however, it is large enough to contain a huge no of molecules so that it can be viewed as a continuous medium. The fluid element may be fixed in space with the fluid moving through it, as shown at the left of fig 3.2. Alternatively, it may be moving along a streamline with a velocity vector V equal to the flow velocity at the each point. Again, instead of looking at the flow field at once, the fundamentals physical principles are applied to just the infinitesimally small fluid element itself. This application leads directly to the fundamental equations. In partial differential equation form. Moreover the particular partial differential equations. Obtained directly from the fluid element fixed in the space is again the conservation form of the equations. The partial differential equations. Obtained directly from the moving fluid element are again called the non-conservation form of the equations.

3.6 Introduction to Governing Equations:

The governing equations for an unsteady, three dimensional, compressible, viscous flow is:

Continuity Equation:

Non conservation form:

Conservation form:

Momentum Equations:

Non conservation form:

X component:

Y component:

Z component:

Conservation form:

X component:

Y component:

Z component:

Energy Equation:

Nonconservation form:

Conservation form:

Compressible Flow

4.1 Introduction:

Compressible flow is defined as that flow in which the density of the fluid does not remain constant during flow. This means that the density changes from point to point in compressible flow.

The examples of compressible flow are as follows:

- i.) flow of gases through orifices and nozzles,
- ii) Flow of gases in machines such as compressors, and
- iii) Projectiles and airplanes flying at high altitude with high velocities, entire the density of the fluid changes during the flow. The change in density of a fluid is accompanied by the changes in pressure and temperature and hence the thermodynamic behavior of the fluids, will have to be taken into account.

Thermodynamic Relations:

The thermodynamic relations have been discussed as follows:

Equation of State: Equation of state is defined as the equations which give the relationship between the pressure, temperature and specific volume of gas. For a perfect gas the equation of state is

$$Pv = RT \quad \dots (4.1)$$

Where P = Absolute pressure in N/
 v = Specific volume or volume per unit mass
 T = Absolute temperature = 273 + (centigrade)
 R = Gas constant in (J/kg K)
 287 J/kg for air.

In equation (2.1), v is the specific volume which is the reciprocal of density

$$V = \frac{1}{\rho}$$

Substituting this value v in equation (4.1), we get

$$\dots (4.2) \quad \mathbf{4.2}$$

Expansion and Compression of Perfect Gas:

When the expansion or compression of a perfect gas takes place, the pressure, temperature and density are changed. The change in pressure, temperature and density of a gas is brought **about** by the processes which are known as

1. Isothermal process and
2. Adiabatic process.

4.2.1. Isothermal process: This is the process in which a gas is compressed or expanded while the temperature is kept constant. The gas obeys Boyle's law, according to which we have

$$Pv = \text{constant, where } v = \text{specific volume} \quad \dots (4.3)$$

4.2.2 Adiabatic process. If the compression or expansion of gas takes place in such a way that the gas gives neither heat, nor takes heat from its surroundings, then the process is said to be adiabatic.

According to this process,

$$p = \text{constant.}$$

Where k = ratio of the specific heat at constant pressure to the specific heat at constant volume

$$k = 1.4 \text{ for air.}$$

The above relation is also written as $p = \text{constant.} \quad \dots (4.4)$

An adiabatic process is reversible (or frictionless), if it is known as isentropic process. And if the pressure and density are related, in such a way that k is not equal to but equal to some positive value then the process is known as polytropic. According to which

$$p = \text{constant} \quad \dots (4.5)$$

Where n but equal to some positive constant.

4.3 Basic Equation of Compressible Flow

The basic equations of the compressible flows are

1. Continuity Equation,
2. Bernoulli's Equation or energy Equation,
3. Momentum Equation,

4.3.1. Continuity Equation: This is based on law conservation of mass which states that matter cannot be created nor destroyed. Or in other words, the matter or mass is constant. For one-dimensional steady flow, the mass per second =

Where ρ = Mass density, A = Area of cross-section, V = Velocity

As mass or mass per second is constant according to law of conservation of mass. Hence

$$\rho AV = \text{constant.} \quad \dots (4.6)$$

Differentiating equation (2.6),

$$d(\rho AV) = 0 \text{ or } d(\rho AV) + \rho AV d = 0$$

$$[A d\rho + \rho dA] + \rho V d = 0$$

Dividing by, we get

$$\frac{d\rho}{\rho} + \frac{dA}{A} + \frac{dV}{V} = 0 \quad \dots (4.7)$$

Equation (2.7) is also known as continuity equation in differential form.

4.3.2. Bernoulli's Equation: The flow of a fluid particle along a streamline in the direction of S is considered. The resultant force on the fluid particle in the direction of S is equated to the mass of the fluid particle and its acceleration. As the flow of compressible fluid is steady, the same Euler's equation is given by

$$\dots (4.8)$$

Integrating the above equation, we get

$$\text{Or } \dots (4.9)$$

In the case of incompressible flow, the density is constant and hence integrating of is equal to. But in the case of compressible flow, the density is not constant. Hence cannot be taken outside the integrating sign. With the change of, the pressure p also changes for compressible fluids. This change of and p takes place according to equations (4.3) or (4.4) depending upon the type of process during compressible flow. The value of from these equations in terms of p is obtained and is substituted in and then the integrating is done. The Bernoulli's equation will be different for isothermal process and for adiabatic process.

(A) Bernoulli's Equation for Isothermal process. For isothermal process, the relation between pressure (p) and density (ρ) is given by equation as

$$= \text{constant} = \dots (i)$$

Substituting the value in Bernoulli's equation, we get

$$\text{Dividing by 'g', } = \text{constant} \dots (4.10)$$

Equation (2.10) is the Bernoulli's equation for compressible flow undergoing isothermal process. For the two points 1 and 2, this equation is written as

$$\dots (4.11)$$

(B) Bernoulli's Equation for Adiabatic process. For the adiabatic process, the relation between pressure (p) and density (ρ) is given by equation (2.4) as

$$= \text{constant} = \text{say} \dots (ii)$$

$$\dots (4.12)$$

4.3.3. Momentum Equations: The momentum per second of a flowing fluid (or momentum flux) is equal to the product of mass per second and the velocity of the flow. Mathematically, the momentum per second of flowing fluid (compressible or incompressible) is

Where =mass per second.

The term is constant at every section of flow due to continuity equation. This means the momentum per second at any section is equal to product of a constant quantity and the velocity. This also implies that momentum per second is independent of compressible effect. Hence the momentum equation for incompressible and compressible fluid for any direction may be expressed as,

Net force in the direction of s=Rate of change of momentum in the direction of

$$s = \text{Mass per second [change of velocity]} = \dots (4.13)$$

Where Final velocity in the direction of Stagnation,
=initial velocity in the direction of S.

Computational Fluid Dynamics

Introduction:

Over the past half-century, we have witnessed the rise in the new methodology for attacking complex problem in fluid mechanics, heat transfer and combustion. It has come to the state that wherever there is a flow, computer can help to understand and analyze the same. This new methodology of solving a flow problem using a computer is given the name CFD. Computational Fluid Dynamics or CFD is the analysis of systems involving fluid flow, heat transfer and associated phenomena such as chemical reactions by means of computer-based numerical approach. In this numerical approach, the equations (usually in partial differential form) that govern a process of interest are solved numerically. The technique is very powerful and spans a wide range of industrial and non-industrial application areas.

5.1 Analysis of a Fluid Flow Problem

There are three methods to analyze a fluid flow problem.

- Experimental
- Theoretical
- Computational (CFD)

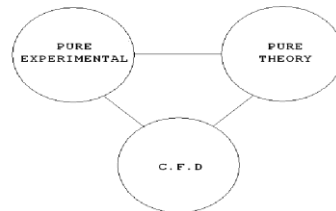


Fig 5.1: The “three dimensions” of fluid dynamics

CFD synergistically complements the other approaches but will never replace either of them. The future advancement of fluid dynamics will rest upon a proper balance of all three approaches, with CFD to interpret and understand theory and experiment and vice versa.

Experimental approach

- Most reliable information
- Full scale tests are prohibitively expensive and often impossible
- The general rules for modeling and extrapolation to full scale are often unavailable
- Simulation of all the features such as combustion or boiling are often omitted from models tests
- Serious difficulties of measurement in many situations
- Measuring instruments have uncertainly errors

Theoretical or Analytical approach

- Solve mathematical models rather than physical models
 - Analytical methods cannot predict many phenomena
 - Analytical or exact solutions are possible only for very simple and ideal situations with many assumptions
- Examples: ideal flows (potential flows), Couette flow, Blassins flow etc.

5.2 Computational Fluid Dynamics:

Advantages

- Low cost, high speed
- Complete information at any inaccessible point
- Ability to simulate realistic conditions and also ideal conditions
- Can handle any complex geometry

Disadvantages

- Proper mathematical model may not be available
- Validation of computer results needs experimental data

Pre-Requisites for CFD

- Fluid mechanics
- Heat transfer
- Partial differential equations
- Numerical methods
- Any programming language with graphical tools.

Approach	Advantages	Disadvantages
----------	------------	---------------

Experimental	1.Capable of being most realistic	1. Equipment required 2. Scaling problems 3.Measurement difficulties 4. Operating costs
Theoretical	1.General information(which is usually in formula form)	1. Restricted to simple geometry and physics 2. Usually restricted to linear problems
Computational	1.No restriction to linearity 2.Complicated physics can be treated 3.Time evolution of flow can be obtained	1. Truncations errors 2. Boundary conditions problems 3. Computer costs

Table 5.1: Comparison of approaches.

5.3 Mathematical Behaviour of Governing Equations in Computational Fluid Dynamics

The development of the high speed digital computer combined with the development of a accurate numerical algorithms for solving problems on these computers has had a great impact on the way principles from the science of Fluid Mechanics are applied to problems of design in modern engineering practice

The physical aspects of any fluid flow are governed by three fundamental principles: conservation of mass, conservation of momentum, conservation of energy and these can be expressed in terms of basic mathematical equations which in their more general form are either integral equations or partial differential equation in computational approach; these equations that govern a process are solved numerically.

These partial differential equations have certain mathematical behavior. This behavior is not fixed and varies from one circumstance to another, depending on the magnitude of the dimensionless flow parameters governing, the situation, the equations governing the flow and the steady or unsteady nature of the flow.

5.4. Discretization:

Introduction:

The word “discretization” requires some explanation. Obviously, it comes from “discrete,” defined in *The American Heritage Dictionary of the English Language* as “constituting a separate thing; individual; distinct; consisting of unconnected distinct parts.” However, the word “discretization” cannot be found in the same dictionary; it cannot be found in *Webster’s New World Dictionary* either. The fact that it does not appear in two of the most popular dictionaries of today implies, at the very least, that it is a rather new and esoteric word. Indeed, it seems to be unique to the literature of numerical analysis, first being introduced in the German literature in 1955 by “W.R. Wasow”, carried on by Ames in 1965 in his classic book on partial differential equations, and recently embraced by the CFD community as closed-for mathematical expression, such as a function or a differential or integral equation involving functions, all of which are viewed as having an infinite continuum of values throughout some domain, is approximated by analogous points or volumes in the domain. This may sound a bit mysterious, so let us elaborate for the sake of clarity. Also, we will single out partial differential equations for the purposes of discussion. Therefore, the remainder of this introductory section dwells on the meaning of “discretization”.

5.4.1. Introduction to Finite Differences:

Here, we are interested in replacing a partial derivative with a suitable algebraic difference quotient, i.e., a *finite difference*. Most common finite-difference representations of derivatives are based on Taylor’s series expansions. For example, if u denotes the x component of velocity at point (i, j), then the velocity at point (i+1, j) can be expressed in terms of a Taylor series expanded about point (i, j) as follows

$$u_{i+1,j} = u_{i,j} + \Delta x \frac{\partial u}{\partial x} + \frac{\Delta x^2}{2!} \frac{\partial^2 u}{\partial x^2} + \dots \quad (5.1)$$

Equation (5.1) is mathematically an exact expression for $u_{i+1,j}$ if the number of terms is infinite and the series converges and/or.

Solving Eq. (5.1) for $\frac{\partial u}{\partial x}$ we obtain

$$\frac{\partial u}{\partial x} = \frac{u_{i+1,j} - u_{i,j}}{\Delta x} - \frac{\Delta x}{2!} \frac{\partial^2 u}{\partial x^2} + \dots \quad (5.2)$$

In Eq. (5.2) the actual partial derivative evaluated at point (i,j) is given on the left side. The first term on the right side, namely $\frac{u_{i+1,j} - u_{i,j}}{\Delta x}$ is a finite-difference representation of the partial derivative. The remaining terms on the right side constitute the *truncation error*. That is, if we wish to *approximate* the partial derivative with the above algebraic finite-difference quotient,

$$\frac{\partial u}{\partial x} \approx \frac{u_{i+1,j} - u_{i,j}}{\Delta x} \quad (5.3)$$

Then the truncation error in Eq. (5.2) tells us what is being neglected in this approximation. In Eq. (5.2), the lowest-order term in the truncation error involves the first power; hence, the finite-difference expression in Eq. (5.3) is called *first-order-accurate*. We can more formally write Eq. (3.2) as

$$\dots (5.4)$$

In Eq. (5.4), the symbol is a formal mathematical notation that represents “terms of order”. Eq. (5.4) is a more precise notation than Eq. (5.3), which involves the “approximately equal” notation. In Eq. (4.4) the order of magnitude of the truncation error is shown explicitly by the notation. In this finite-difference expression in Eq. (5.4) uses information to the *right* of grid point (i, j); that is, it uses as well as. No information to the left of (i, j) is used. As a result, the finite difference in Eq. (3.4) is called a *forward difference*. For this reason, we now identify the first-order-accurate difference representation for the derivative expressed by Eq. (5.4) as a *first-order forward difference*, repeated below.

$$\dots (5.4)$$

Let us now write a Taylor expansion for , expanded about

Or

$$\dots (5.5)$$

Solving for, we obtain

$$\dots (5.6)$$

The information used in forming the finite-difference quotient in Eq. (5.6) comes from the *left* of grid point (i, j); that is, it uses as well as. No information to the right of (i, j) is used. As a result, the finite difference in Eq. (5.6) is called a *rearward (or backward) difference*. Moreover, the lowest-order term in the truncation error involves to the first power. As a result, the finite difference in Eq. (5.6) is called a *first-order rearward difference*. In most application in CFD, first-order accuracy is not sufficient. To construct a Finite-difference quotient of second-order accuracy, simply subtract Eq. (5.5) from Eq. (5.1)

$$\dots (5.7)$$

Eq. (5.7) can be written as

$$\dots (5.8)$$

The information used in forming the finite-difference quotient in Eq. (3.8) comes from *both* sides of the grid point located at (i, j); that is, it uses as well as. Grid point (i, j) falls between the two adjacent grid points. Moreover, in the truncation error in Eq. (5.7), the lowest-order terms involves, which is second-order accuracy. Hence, the finite-difference quotient in Eq. (5.8) is called a *second-order central difference*.

Difference expression for the ‘y’ derivatives is obtained in exactly the same fashion. The results are directly analogous to the previous equations for the x derivatives. They are:

Eq’s. (5.4, 5.6) & (5.8 to 5.11) are examples of finite-difference quotients for first partial derivatives. Note that the highest-order derivatives which appear in the Euler equations are first order partial derivatives. Hence, finite differences for the first derivatives, such as those expressed by Eq’s (5.4, 5.6&5.8) are all that we need for the numerical solution of in-viscid flows. On the other hand, if we are dealing with viscous flows, the governing equations are the Navier-Stokes equations. Note that the highest-order derivatives which appear in the Navier-stokes equations are *second* order partial derivatives, as reflected in the viscous terms such as &. When expanded, these terms involve such second partial derivatives as &. Consequently, there is a need for discretizing second-order derivatives for CFD. We can obtain such finite-difference expressions by continuing with a Taylor series analysis, as follows.

Summing the Taylor series expansion given by Eq. (3.1 & 3.5), we have

Solving for

$$\dots (5.12)$$

In eq. (5.12), the first term on the right-hand side is a central finite difference for the second derivative with respect to x evaluated at grid point (i, j); from the remaining order-of-magnitude term, we see that this central difference is of second-order accuracy. An analogous expression can easily be obtained for the second derivative with respect to y, with the result that

$$\dots (5.13)$$

Eq’s. (5.12 & 5.13) are the examples of second-order central second differences.

5.5 Explicit and Implicit Approaches:

5.5.1 Definitions and Contrasts:

We have discussed some basic elements of the finite –difference method. We have done nothing more than just create some numerical tools for future use; we have not yet described how these tools can be put to use for the solutions of CFD problems. The way that these tools are put together and used for a given solution can be called a CFD *technique*, and we have not yet discussed any specific techniques. However, once you choose a specific technique to solve your given problem, you will find that the technique falls into one or the other of two different general approaches, an *explicit* approach or an *implicit* approach. It is appropriate to introduce and define these two general approaches now; they represent a fundamental distinction between various numerical techniques, a distinction for which we need to have some appreciation at this stage of our discussion. For simplicity, let us return to the one-dimensional equation given by Eq. (5.a) repeated below.

..... (5.a)

We will treat Eq. (5.a) as a “model equation” for our discussion in this section; all the necessary points concerning explicit and implicit approaches can be made using this model equation without going to the extra complexity of the governing flow equations. Above, we used Eq. (5.a) to illustrate what was meant by a difference equation. In particular, in that section we choose to represent with a forward difference and with a central second difference, leading to the particular form of the difference equation given by Eq. (5.18) repeated below:

..... (5.18)

With some rearrangement, this equation can be written as

..... (5.19)

Let us examine the implications of Eq. (5.a) and its difference equation counterpart given by Eq. (5.19). It is a parabolic partial differential equation. Being parabolic, this equation lends itself to a marching solution. The marching variable here is time ‘t’. To be more specific, consider the finite-difference grid sketched in fig. Assume that V is known at all grid points at time level n. Time marching means that ‘V’ at all grid points at time level n+1 are calculated from the known values at time level n. when this calculation is finished, we have known at time level n+1. Then the same procedure is used to calculate ‘V’ at all grid points at tie level n+2, using the known values at level n+1. In this fashion, the solution is progressively obtained by marching in steps of time. Casting our attention to Eq. (5.19) we see a straight forward mechanism to accomplish this time marching. Notice that Eq. (5.19) is written with properties at time level n on the right-hand side and properties at time level n+1 on the left-hand side.

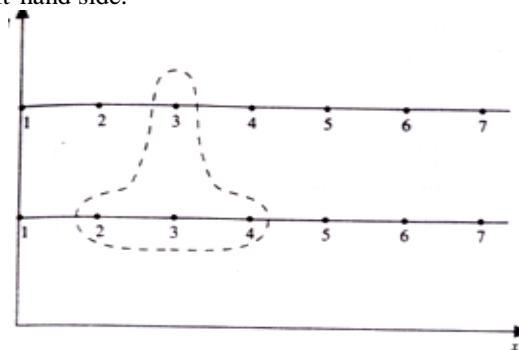


Fig 5.2 An explicit finite difference module

Recall that, within the time-marching philosophy, all properties at level n are known and those at level n+1 are to be calculated. Of particular significances is that only one unknown appears in Eq. (5.19) namely. Hence Eq. (5.19) allows for the immediate solution of from the known properties at time level n. we have a single equation with a single unknown-nothing could be simpler. For example, consider the grid shown in fig. (5.3) where we choose to distribute seven grid points along x-axis. Centering on grid point 2, Eq. (5.19) is written as

..... (5.20)

This allows the direct calculation of since the quantities on the right-hand side of Eq. (3.20) are all known numbers. Then, centering on grid point 3, Eq. (3.19) is written as

..... (5.21)

This allows the direct calculation of from the known numbers on the right-hand side of Eq. (5.21) In the same vein, by sequential application of Eq. (5.19) to grid points 4, 5, 6, we obtain sequentially,, &. What we have just presented in the above paragraph is an example of an *explicit* approach. By definition, in an explicit approach each difference equation contains only one unknown and therefore can be solved explicitly for this unknown in a straightforward manner. Nothing could be simpler. This explicit approach is further illustrated

by finite-difference module within the dashed balloon in (Fig 5.3). Here, the module contains only one unknown at time level $n+1$.

In regard to grid points 1 and 7 in fig. (5.3) the marching solution of a parabolic partial differential equation presupposes the stipulation of boundary conditions. In regard to fig. (5.3) this means that u_1 and u_7 , which represent V at the left and right boundaries, respectively, are known numbers at each time level, known from the stipulated boundary conditions. Eq. (5.18) is not only difference equation that can represent Eq. (5.a) in fact; it is only one of many different representations of the origin partial differential equation. As a counter example to the above discussion concerning the explicit approach.

Let us be somewhat return to Eq. (5.a) this time writing the spatial difference on the right-hand side in terms of *average* properties between time levels ' n ' and ' $n+1$ '. That is, we will represent Eq. (5.a) by

$$\dots (5.22)$$

The special type of differencing employed in Eq (5.22). is called "*Crank-Nicholson form*". (Crank-Nicholson differencing is commonly used to solve problems governed by parabolic equations, In CFD, the Crank-Nicholson form, or modified versions of it, is used frequently for finite-difference solutions of the boundary-layer equations.) Examine Eq. (5.22) closely. The unknown u_i^{n+1} is not only expressed in terms of the known quantities at time level ' n ', namely $u_1^n, u_2^n, u_3^n, u_4^n, u_5^n, u_6^n, u_7^n$, but also in terms of other unknown quantities at time level ' $n+1$ ', namely, u_{i-1}^{n+1} and u_{i+1}^{n+1} . In other words, Eq. (5.22) represents one equation with *three* unknowns, namely, u_{i-1}^{n+1}, u_i^{n+1} , and u_{i+1}^{n+1} . Hence, Eq. (5.22) applied at a given grid point ' i ' does not stand alone; it cannot by itself result in a solution for u_i^{n+1} . Rather Eq. (5.22) must be written at all grid points, resulting in a *system* of algebraic equations from which the unknowns u_i^{n+1} for all ' i ' can be solved simultaneously. This is an example of an implicit approach. By definition, an implicit approach is one where the unknowns must be obtained by means of simultaneous *solution* of the difference equation applied at all grid points arrayed at a given time level. Because of this need to solve large systems of simultaneous algebraic equations, implicit methods are usually involved with the manipulations of large matrices. By now, it is easy to get the feeling that the implicit approach involves a more complex set of calculations than the explicit approach discussed earlier. In contrast to the simple explicit finite-difference module shown in fig.(5.a1), the implicit module for Eq. (5.22) is sketched in fig.(5.a2) clearly delineating the three unknowns at level $n+1$.

Let us be more specific, using the seven-point spatial grid shown in fig. (5.a2) as an example. Equation can be rearranged to display the unknown and the left-hand side and the known on the right-hand side. The result is

$$\dots (5.23)$$

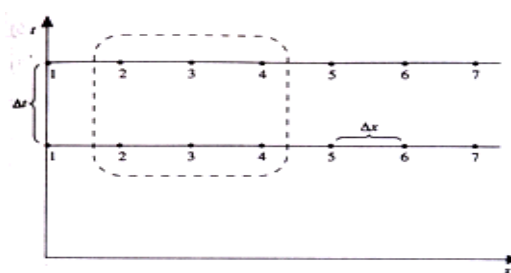


Fig 5.3 An implicit finite difference module

Simplifying the nomenclature by denoting the following quantities by A, B, and

We can write the Eq. (5.23) in the form

$$\dots (5.24)$$

Note that ' u_i^n ' in Eq. (5.24) consists of properties at time level ' n ', which are known. Hence, ' u_i^n ' is a known number in Eq. (5.24) Returning to fig.(5.a2), we now apply Eq. (5.24) sequentially to grid points '2' through '6'.
At grid point 2:

$$\dots (5.25)$$

Here, we have dropped the superscript for convenience; it is easy to remember that u_i represent three values at time level ' $n+1$ ', and u_i^n is a known number as stated before. Moreover, because of the stipulated

boundary conditions at grid points '1' and '7', in Eq. (5.25) is a known number. Hence, in Eq. (5.25) the term involving the known can be transferred to the right-hand side, resulting in

$$\dots (5.26)$$

Denoting by θ , where θ is a known number, Eq. (3.26) is written as

$$\dots (5.27)$$

At grid point 3:

$$\dots (5.28)$$

At grid point 4:

$$\dots (5.29)$$

At grid point 5:

$$\dots (5.30)$$

At grid point 6:

$$\dots (5.31)$$

In Eq. (5.31) since grid point 7 is on a boundary, θ is known from the stipulated boundary condition. Hence, Eq. (5.31) can be rearranged as

$$\dots (5.32)$$

Where θ is a known number

5.5.2 Explicit Approach

- Advantage: Relatively simple to set up and program.
 Disadvantage: In terms of our above example, for a given x , t must be less than some limit imposed by stability constraints. In some cases, Δt must be very small to maintain stability; this can result in long computer running times to make calculations over a given interval of t .

5.5.3 Implicit Approach

- Advantage: stability can be maintained over much larger values of ' t ', hence Using considerable fewer time steps to make calculations over a given interval of ' t '. This results in less computer time.
 Disadvantage: more complicated to set up and program.
 Disadvantage: since massive matrix manipulations are usually required at each time step, the computer time per time step is much larger than in the explicit approach.
 Disadvantage: since large ' t ' can be taken, the truncation error is large, and the use of implicit methods to follow the exact transients (time Variations of the independent variable) may not be as accurate as an explicit approach. However, for a time-dependent Solution in which the steady state is the desired result, this relative time wise inaccuracy is not important.

5.6 Finite Volume:

Finite volume method is one of the very popular approximate methods to solve the governing equations originated from fluid dynamics. The governing equations discretized using this method may resemble similar to the equations discretized with finite difference method but the basic idea behind these two schemes is very different. In general, in finite difference method, the mathematically modeled differential or integral equations are taken as the correct and appropriate form of the conservation principles governing the physical problem and then making use of Taylor series or integral methods the differential or integral equations are converted into algebraic form. However, in finite volume method, after discretizing the domain under consideration as sub-domains called control volumes, the conservation statements are applied in each of these control volumes. That is, the conservation principles are made to satisfy in each of the control volumes. The generation of control volumes can be done in two ways

1. *Cell-Centered method:* In this method, the control volumes are identified first and then grid points will be placed at the center of each cell.
2. *Cell-Vertex method:* In cell vertex method the grid points will be identified first and then the boundaries of the control volume are fixed at half way between the grid points. If the grid points are identified non-uniformly in this scheme then these points need not be at the geometric centre of the control volumes.

5.7 MacCormack's Technique

MacCormack's technique is a variant of the lax-Wendroff approach but is much simpler in its application. Like the Lax-Wendroff method, the MacCormack method is also an explicit finite-difference technique which is second order accurate in both space and time. First introduced in 1969, it became the most popular explicit finite difference method for solving fluid flows for the next 15 years. Today, the MacCormack method has been mostly supplanted by more sophisticated approaches. However, the understand and program. Moreover, the results obtained by using MacCormack's method are perfectly satisfactory for many fluid flow applications.

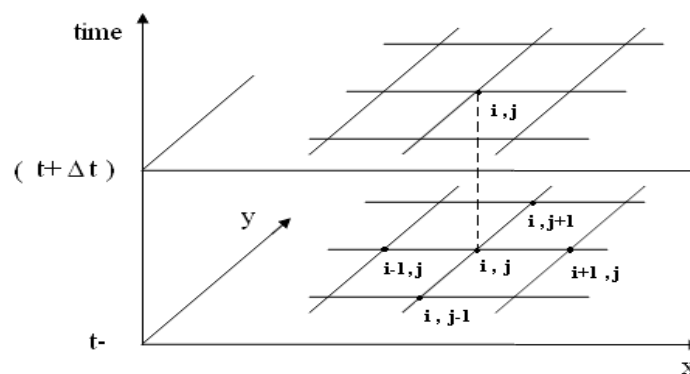


Fig 5.4: A schematic of the grid for time marching

Consider again two dimensional grid show in fig 'a'. For purpose of illustration, let us address again the solution of the Euler equations itemized. Here we discussed a time marching solution using the Lax Wendroff technique. Here, we will address a similar time marching solution but using MacCormack's technique. As before, we assume that the flow field at each grid point in fig 'a' is known at time 't' and we proceed to calculate the flow field variables at the same grid points at time (t+t), as illustrated fig 'b'. First consider the density at grid point (i, j) at time (t+t). In MacCormack's method, this obtained from

$$(5.33)$$

Where $\bar{\rho}$ is a representative mean value of between times t and (t+t). The value of $\bar{\rho}$ is calculated so as to preserve second order accuracy without the need to calculate values of the second time derivatives which involves lot of algebra. With MacCormack's technique this algebra is circumvented. Similar relations are written for the other flow field variables.

$$(5.34)$$

$$(5.35)$$

$$(5.36)$$

Let us illustrate by using the calculation of density as an example. The average time derivative is obtained from a predictor corrector philosophy as follows.

5.7.1 Predictor step:

In the continuity equation replace the spatial derivatives on the right hand side with forward differences.

$$(5.37)$$

In the above equation, all flow variables at time t are known values; i.e., the right hand side is known. Now obtain a predicted values of density, from the first two terms of a Taylor series, as follows.

(5.38)

In the above equation, ρ is known, and ρ_{old} is known number and hence ρ_{new} is readily obtained. The value of ρ_{new} is only a *predicted value* of density; it is only first order accurate since contains only the first order term in Taylor series. In a similar fashion, predicted values for u , v , and e can be obtained, i.e.

(5.39)

(5.40)

(5.41)

In equations (5.39) to (5.41), numbers for the time derivatives on the right hand side are obtained from continuity equations, respectively, with forward differences used for the spatial derivatives, similar to those shown in equation (5.37) for continuity equation

5.7.2 Corrector Step:

In the corrector step, first we obtain a predicted value of the time derivatives at time

Derivative at time $t+\Delta t$ by substituting the predicted values of u , v , and e into right hand side of the continuity equation, replacing the spatial derivatives with forward differences.

(5.42)

The average values of the time derivative of density which appears in equation (4.33) is obtained from the arithmetic mean of left hand side, obtained from equation (4.37) and left hand side, obtained from equation (4.42).

(5.43)

This allows us to obtain the final, “corrected value of the density at time $t+\Delta t$ from equation (1), repeated below:

(5.44)

MacCormack’s technique as described above, because a two step predictor – corrector sequence is used with forward differences on the predictor and with backward differences on the corrector, is a second-order-accurate method. Therefore, it has the same accuracy as the Lax Wendroff method. However, the MacCormack method is much easier to apply.

Design and CFD Analysis of Radiator Fan Assembly

6.1 Outline:

- Background
- Problem statement
- Design
- Problem setup
- Meshed model
- Boundary conditions
- Results

6.2 Background:

The extended use of axial flow fans for fluid movement and heat transfer has resulted in detailed research into the performance attributes of many designs [1], [2]. Numerical investigations have been performed to quantify the performance of axial fans and their flow characteristics

Fans can be radial or axial. For large volume flows and low pressure increase axial fans are preferred if the total pressure increase is very low, the rotor looks like a propeller. Axial fans are also used when the radial space is restricted. Radial Fans Radial fans (or blowers) are the most common ones used ones. The blades can be arranged straight ones in the radial direction, which is said to make the fan useful for gases contaminated with particles. They use a rotating impeller to move the air stream, increasing its

velocity. The speed increases as it reaches the ends of the blades and is then converted to an increase in pressure. These fans can work under high temperatures and high pressurized conditions. Axial fans are normally used for cooling systems, since they allow large volume flows and low pressure increase. If the total pressure increase is very low, the rotor looks like a propeller. Axial fans are also used when the available radial space is restricted. The blades in axial fans are mostly formed as wing profiles. To get a good efficiency, they should be skewed in the radial direction they work by moving an air stream along the axis of the fan. It can be compared to a propeller on an airplane: the fan blades generate an aerodynamic lift that pressurizes the air. They are inexpensive, compact and light which makes them the best choice for the cooling systems. The highest total efficiency is obtained with blades curved backward, even though they do not achieve an energy conversion as high as forward blades. However, this type of fan operates stably because the pressure difference provided by the fan drops if the flow rate goes up. If the opposite were true, an increased flow rate would cause increase fan power, which would be unstable. This gives them the design advantage that makes them the best choice for the bus cooling systems.

6.3 Problem Statement:

The efficiency of automotive radiator is largely dependent on the ability of the fan to force the air draught as much as possible. In order to devise an effective fan design, the primary objective is to maintain desired pressure difference between the fan inlet and outlet.

The radiator fan design was first evaluated through simulations to obtain pressure difference and torque values. In order to obtain the desired pressure difference and torque.

The radiator fan with 12 blades was first analyzed through CFD simulations and the pressure difference between the fan inlet and outlet were measured. To improve performance keeping the same number of blade and discharge with changing the rotational speed of the fan were suggested and flow analysis for the same was performed. Desired pressure difference was obtained through the various rotational speeds. Final results show better efficiency calculating by the numerical simulation. This solution can also be provided using FLUENT.

6.4 Design:

The first step is to identify a typical radiator axial flow fan that can be reproduced as a 3-D CAD Solidworks® software engineering drawing package (Fig. 5). The 3-D models are then imported into the CFD software, remodeled into different sections, and refined to generate a finite volume meshing (Fig. 6). This is a crucial step, where details of the geometrical shape need to be defined precisely. The flow domain is also created, and the final meshing of all components needs to be accurate. The total element count will be around 1.6 million, with an inflation layer on the blades. Any errors in the drawings and flow area need to be corrected before continuing.

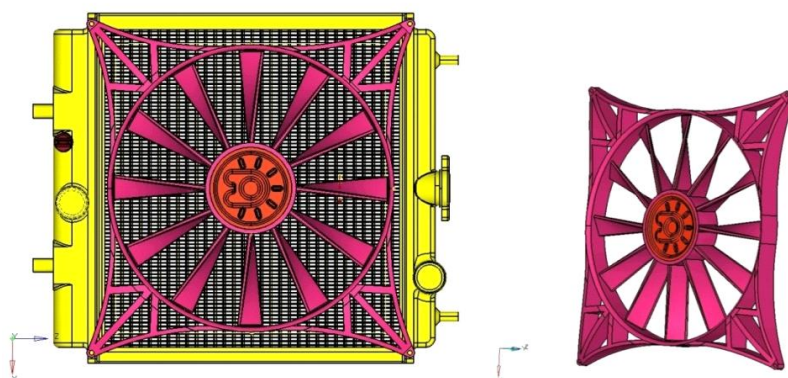


Fig. 5 Computational domain of a fan

The second step is to import the files into the CFD code preprocessor, which will solve the flow equations. Here, the flow fields boundary conditions are set. These include inlet air mass flow, outlet pressure, fluid properties, and flow domain characterization, such as moving internal zone and stationary solid walls. The next step is to set the simulation process as a 3-D steady and turbulent problem.

FAN-SHROUD Assembly Specifications:

Specification

Number of Blades	12
Fan Diameter	300 mm
Blade Thickness	4.25mm
Height of the blade	100mm
Hub outer diameter	100mm
Hub Thickness	37mm
Rotation	CW from Front End

FAN-Geometry and Domains

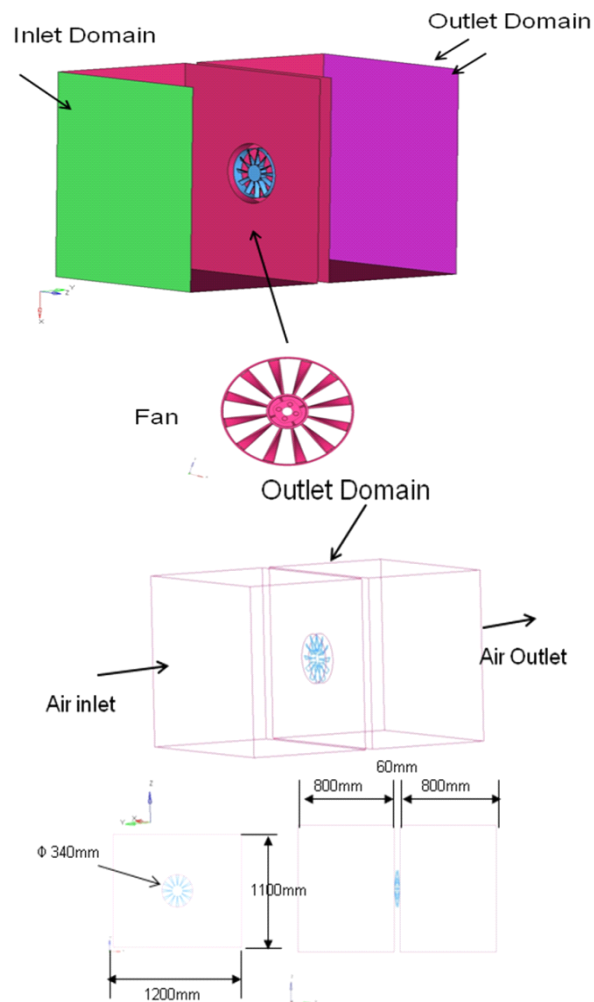


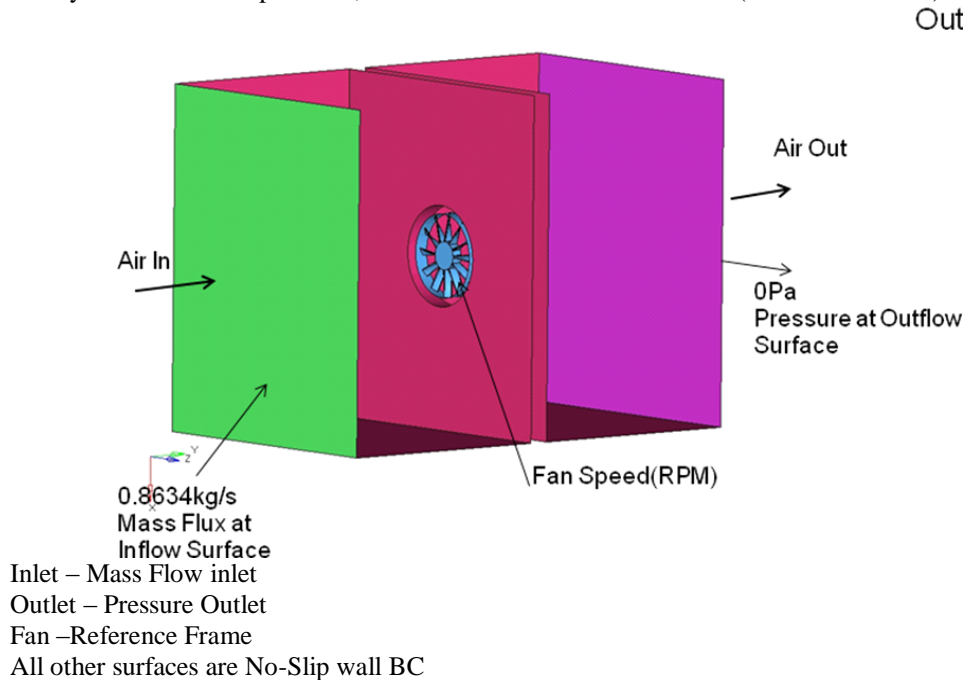
Fig. 6 FAN-Geometry and Domains

6.5 Problem setup:

For the steady RANS simulations, the single equation Spalart-Allmaras (SA) turbulence model was used. The turbulence equation is solved segregated from the flow equations using the GLS formulation. Reference Frame is used to simulate the Rotating Flow

6.6 Boundry Conditions:

The outlet has been modeled with static pressure of 1 atm. Spalart-Allmaras (SA) Turbulence model was used. High Resolution Option was employed for all transport equations. The convergence criteria were a normalized RMS residual on all variables of 1.0×10^{-4} , and a 'Conservation target' (i.e. global balance) of 1.0×10^{-3} . In convergence controls auto time scaling was employed with conservative length scale option. Type of flow is Steady-state and Incompressible, all wall modeled as adiabatic wall (No Heat Transfer) with no slip condition



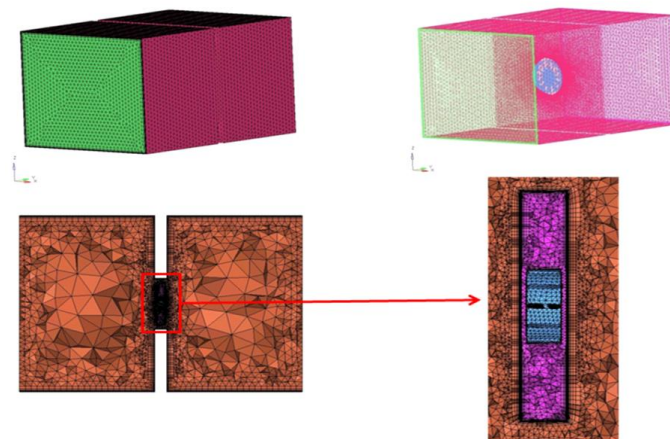
Boundary conditions summary:

S. No	Inlet:(Mass flow rate(kg/s))	Outlet:(Pressure (Pa))	RPM
case1	0.8634	0	2700
case2	0.8634	0	3000
case3	0.8634	0	3300
case4	0.8634	0	3600

6.7 Meshed Model-1:

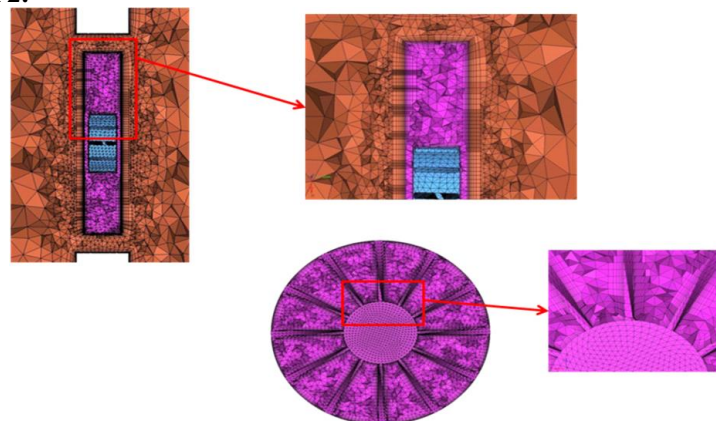
Once the geometry has been the defined, the fluid region of the domain is then filled with elements, forming a computational mesh. The relevant equations are then solved at the vertices (or corners) of these elements, yielding velocities, pressures, temperatures, concentrations, etc. In this case the tetrahedral element type (four triangular faces, four vertices) is used. Hyper mesh 12.0 was used for Meshing.

In this case the complete mesh consisted of ~1 million tetrahedral volume elements with 10 layer of the boundary layer. The size of this computational mesh is sufficient to adequately resolve the features of importance. Surface mesh for various parts and vertical section through volume mesh are shown in the following Figures



Total number of cells ~954261

6.8 MESHED Model 2:



Total number of boundary layers--10

Results and Discussions

On Post processing the numerical CFD results, the observations are presented as velocity vector distributions, flow lines and static pressure contour plot at mid section of the fan and also on rotor. For the velocity vector representation, a plane is taken normal to the y-axis coordinate and at the centre (0, 0, 0). Results are compiled separately for the front and back oriented blades

7.1. Analysis results for Case-1, 2700 RPM

Fig. 7.1a, illustrates the velocity magnitude on the rotor, which confirms that velocity increased moving from the hub to the tip on the rotor and thus validated the theoretical concept of $V = r \cdot \omega$. This also affirms that the rotor was rotating at the center point of the fan axis. maximum tip velocity is 40.53m/s.

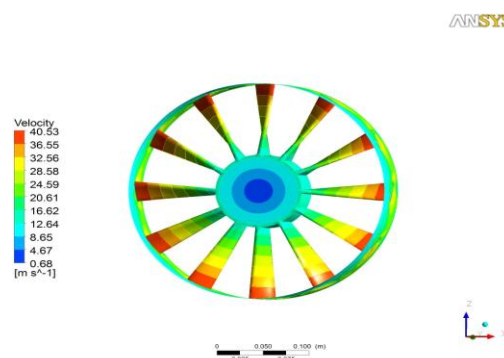


Fig. 7.1a Velocity magnitude on rotor

Figs. 7.1b show the velocity vector distribution, at a plane normal to the y-axis (mid of the rotor). A high flow region formed around the outer diameter of the flow domain and a low reverse flow region formed in the center

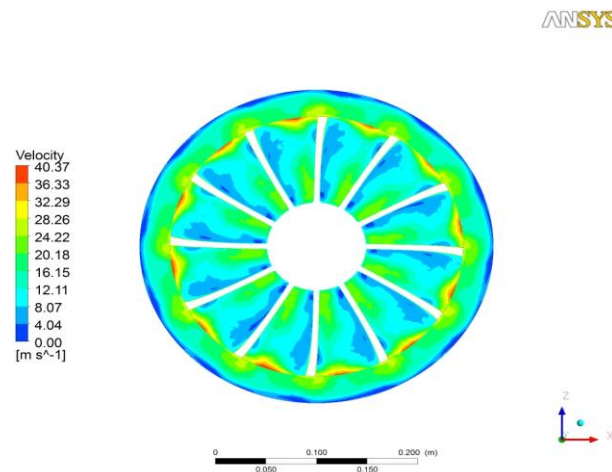


Fig. 7.1b Velocity magnitude at mid plan of the rotor

behind the fan hub. Between the high and low reverse flow regions, there existed strong circulation vortices. Strong circulation regions were also observed behind the fan blades. This helps in understanding the flow behavior around the rotor.

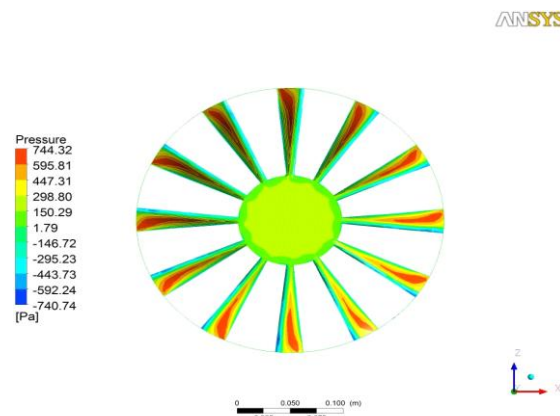


Fig. 7.1c Static pressure on rotor

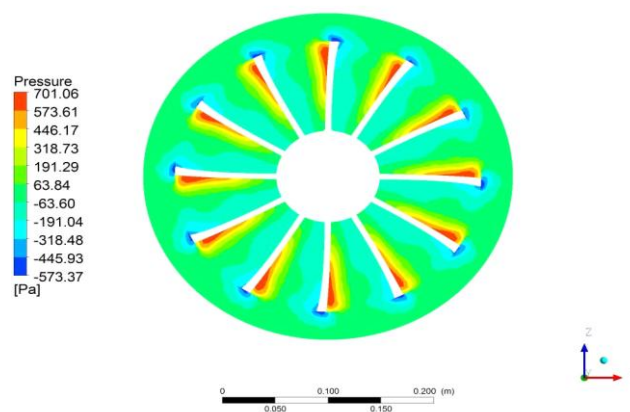


Fig. 7.1d Static pressure at mid plan of the rotor

Figs. 7.1c and 7.1d, show the pressure contours for static pressure at mid plane of the rotor and on rotor. By observing the pressure contour at the rotor, pressure varies from -740.74 pa to 744.32Pa.

ANSYS

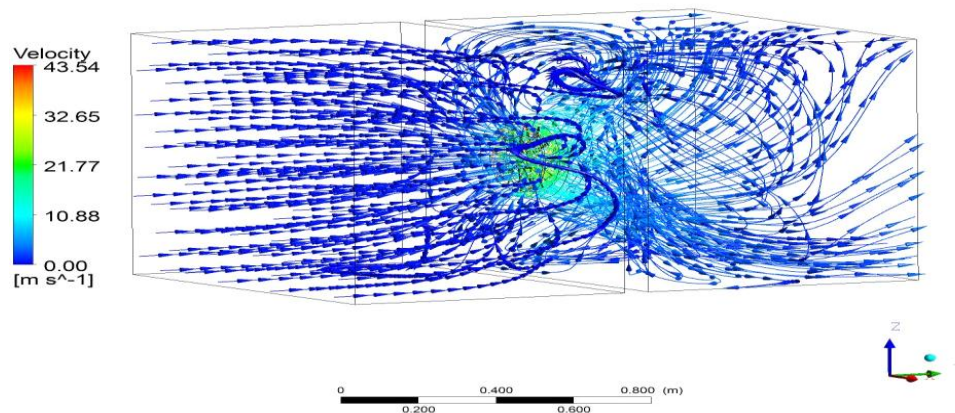


Fig. 7.1e Stream line

Fig.7.1e show the velocity distribution of streamlines from inlet to outlet of the domain. Again, a high flow region formed around the outer diameter of the flow domain (i.e., at the tip side of the blade). Also, a low reverse flow region formed in the center behind the fan hub. There existed strong circulation vortices in between the high and low reverse flow regions.

7.2. Analysis results for Case-2, 3000 RPM

Fig. 7.2a, illustrates the velocity magnitude on the rotor, which confirms that velocity increased moving from the hub to the tip on the rotor and thus validated the theoretical concept of $V = r\omega$. This also affirms that the rotor was rotating at the center point of the fan axis. maximum tip velocity is 45.04m/s.

ANSYS

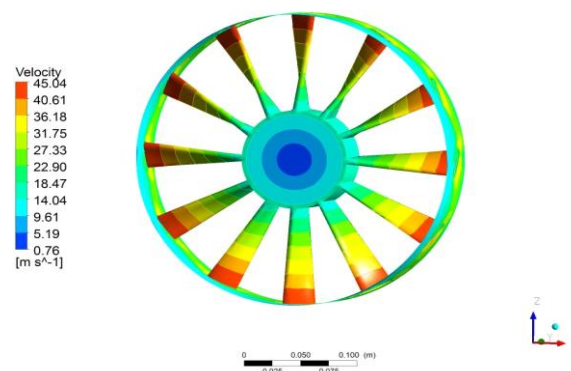


Fig. 7.2a Velocity magnitude on rotor

Figs. 7.2b show the velocity vector distribution, at a plane normal to the y-axis (mid of the rotor). A high flow region formed around the outer diameter of the flow domain and a low reverse flow region formed in the center

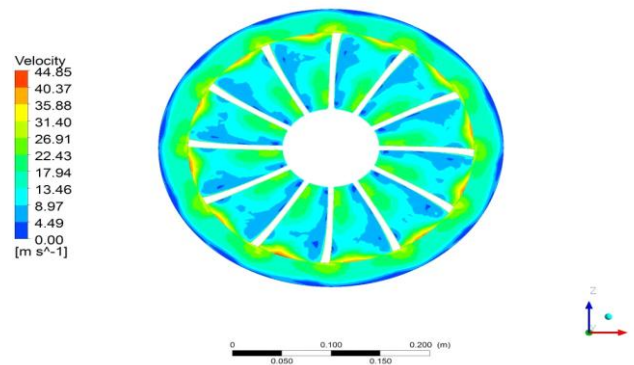


Fig. 7.2b Velocity magnitude at mid plan of the rotor

behind the fan hub. Between the high and low reverse flow regions, there existed strong circulation vortices. Strong circulation regions were also observed behind the fan blades. This helps in understanding the flow behavior around the rotor.

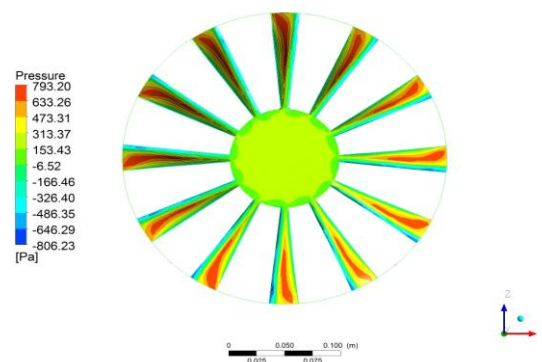


Fig. 6.2c Static pressure on rotor

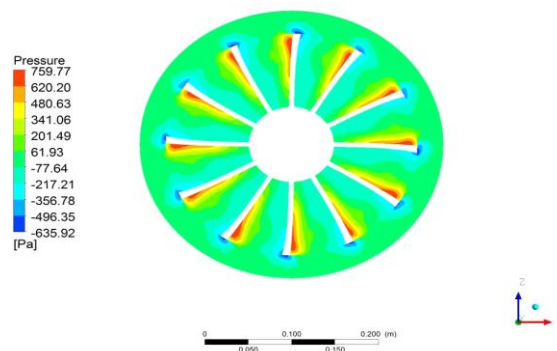


Fig. 7.2d Static pressure at mid plan of the rotor

Figs. 7.2c and 7.2d, show the pressure contours for static pressure at mid plane of the rotor and on rotor. By observing the pressure contour at the rotor, pressure varies from -806.23 pa to 793.2Pa.

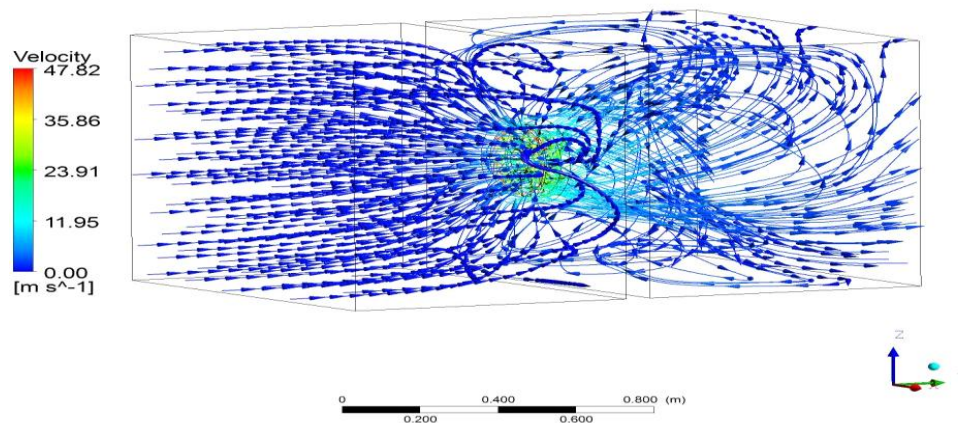


Fig. 7.2e Stream line

Fig.7.2e show the velocity distribution of streamlines from inlet to outlet of the domain. Again, a high flow region formed around the outer diameter of the flow domain (i.e., at the tip side of the blade). Also, a low reverse flow region formed in the center behind the fan hub. There existed strong circulation vortices in between the high and low reverse flow regions.

7.3. Analysis results for Case-3, 3300 RPM

Fig. 7.3a, illustrates the velocity magnitude on the rotor, which confirms that velocity increased moving from the hub to the tip on the rotor and thus validated the theoretical concept of $V = r \cdot \omega$. This also affirms that the rotor was rotating at the center point of the fan axis. maximum tip velocity is 49.54m/s.

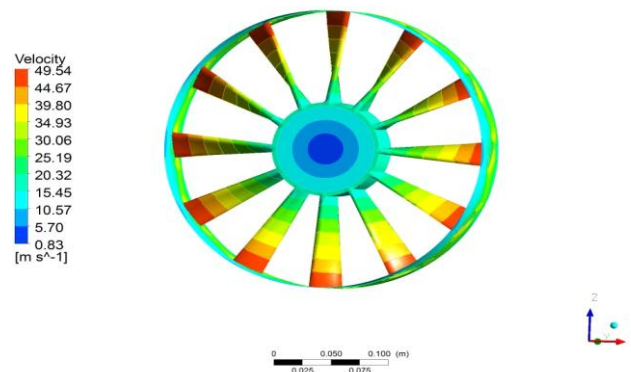


Fig. 7.3a Velocity magnitude on rotor

Figs. 7.3b show the velocity vector distribution, at a plane normal to the y-axis (mid of the rotor). A high flow region formed around the outer diameter of the flow domain and a low reverse flow region formed in the center

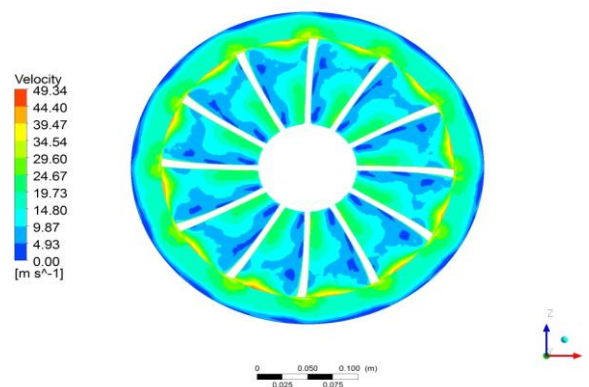


Fig. 7.3b Velocity magnitude at mid plan of the rotor

behind the fan hub. Between the high and low reverse flow regions, there existed strong circulation vortices. Strong circulation regions were also observed behind the fan blades. This helps in understanding the flow behavior around the rotor.

ANSYS

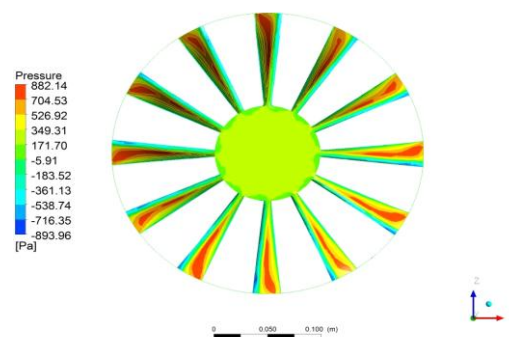


Fig. 7.3c Static pressure on rotor

ANSYS

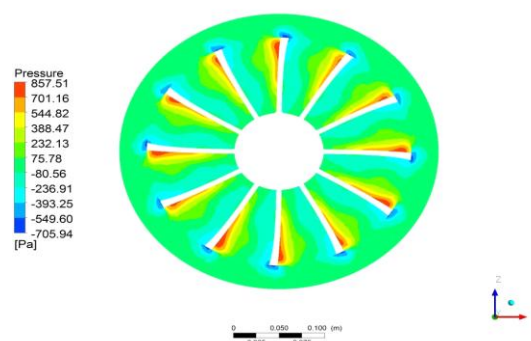


Fig. 7.3d Static pressure at mid plan of the rotor

Figs. 7.2c and 7.2d, show the pressure contours for static pressure at mid plane of the rotor and on rotor. By observing the pressure contour at the rotor, pressure varies from -893.96 Pa to 882.14 Pa.

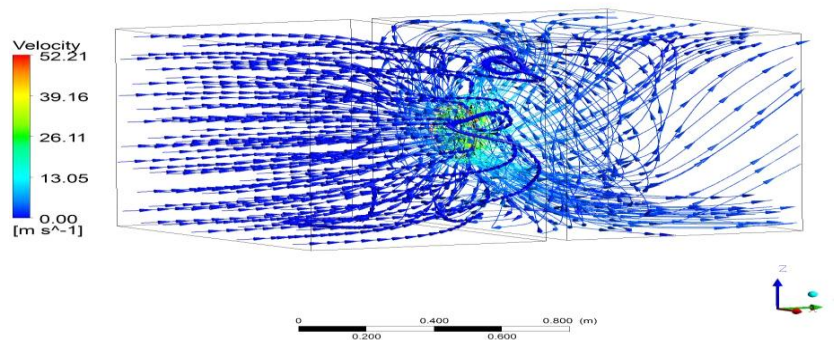


Fig. 7.3e Stream line

Fig.7.3e show the velocity distribution of streamlines from inlet to outlet of the domain. Again, a high flow region formed around the outer diameter of the flow domain (i.e., at the tip side of the blade). Also, a low reverse flow region formed in the center behind the fan hub. There existed strong circulation vortices in between the high and low reverse flow regions.

7.4. Analysis results for Case-4, 3600 RPM

Fig. 7.4a, illustrates the velocity magnitude on the rotor, which confirms that velocity increased moving from the hub to the tip on the rotor and thus validated the theoretical concept of $V = r \cdot \omega$. This also affirms that the rotor was rotating at the center point of the fan axis. maximum tip velocity is 54.04m/s.

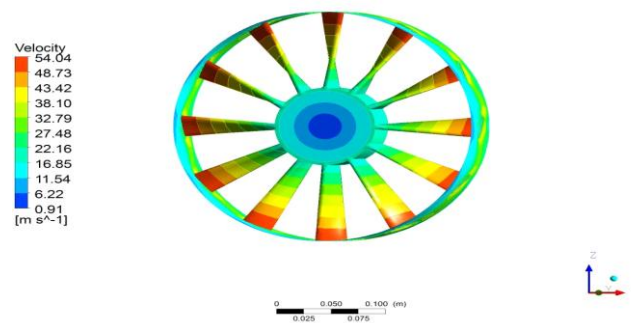


Fig. 7.4a Velocity magnitude on rotor

Figs. 7.4b show the velocity vector distribution, at a plane normal to the y-axis (mid of the rotor). A high flow region formed around the outer diameter of the flow domain and a low reverse flow region formed in the center

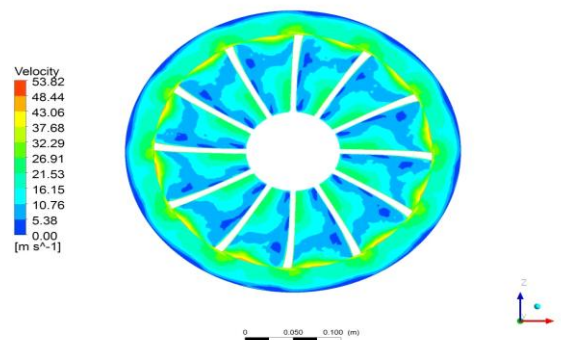


Fig. 7.4b Velocity magnitude at mid plan of the rotor

behind the fan hub. Between the high and low reverse flow regions, there existed strong circulation vortices. Strong circulation regions were also observed behind the fan blades. This helps in understanding the flow behavior around the rotor.

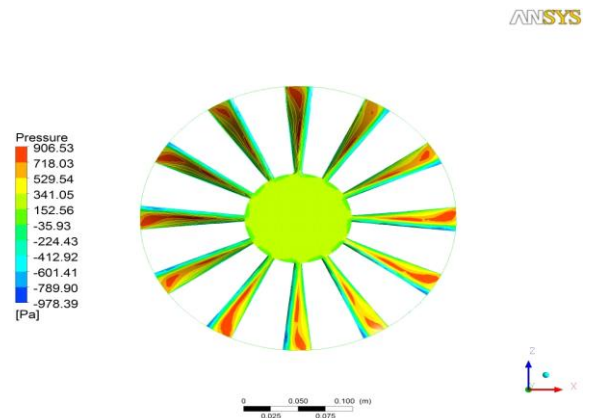


Fig. 7.4c Static pressure on rotor

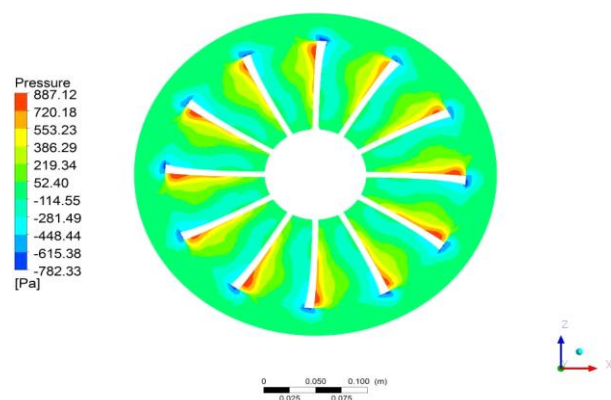


Fig. 7.4d Static pressure at mid plan of the rotor

Figs. 7.4c and 7.4d, show the pressure contours for static pressure at mid plane of the rotor and on rotor. By observing the pressure contour at the rotor, pressure varies from -978.39 Pa to 906.53 Pa.

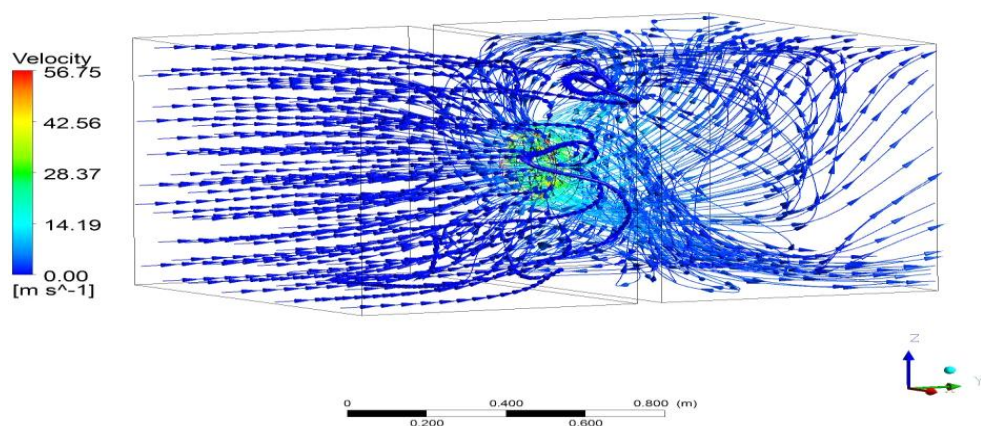


Fig. 7.4e Stream line

Fig.7.4e show the velocity distribution of streamlines from inlet to outlet of the domain. Again, a high flow region formed around the outer diameter of the flow domain (i.e., at the tip side of the blade). Also, a low reverse flow region formed in the center behind the fan hub. There existed strong circulation vortices in between the high and low reverse flow regions.

Pressure losses are calculated for different load cases and are presented below.

Pressure drop for the three load cases:



S. No	Mass flow rate(kg/s)	Blade speed(RPM)	Delta Pressure(Pa)
Case1	0.8634	2700	163.215
Case2	0.8634	3000	168.356
Case3	0.8634	3300	195.055
Case4	0.8634	3600	189.072

Conclusions and Future Work

The results from the numerical simulations provided an insightful understanding of the behavior of fluid flow around the different fan blade speeds. Numerical CFD analysis was performed for a fan with a 2700,3000,3300and 3600 RPM blade speeds. The numerical CFD results were then compared between the various speeds. The key and important outcomes of this study are as follows

- In this work numerical simulation was performed for radiator fan. CFD results to study flow distribution and back pressure estimate. Velocity magnitude, pressure contours & steam line shows flow characteristics that help to understand and verify the main vortex structures found by CFD. Based on this simulation the following conclusions were reached. Radiator fan best operating speed was 3300rpm.
- The CFD modeling shown in this study proved to be very helpful in initiating further and more comprehensive numerical study of the off-road engine cooling system.
- CFD results were presented in the form of velocity contours and stream lines, which provided actual flow characteristics of air around the fan for different blade orientations

Reference

- [1]. Yiding Cao and KhokiatKengskool, “An Automotive Radiator Employing Wickless Heat Pipes” Florida International University, Miami, Conference Paper, 1992.
- [2]. Hwa-Ming Nieh, Tun-Ping Teng, Chao-Chieh Yu “Enhanced heat dissipation of a radiator using oxide nano-coolant”. International Journal of Thermal Sciences 77, 252-261, 2014.
- [3]. M.Naraki and S.M. Peyghambarzadeh, “Parametric study of overall heat transfer coefficient of CuO/water Nano fluids in a car radiator”. International Journal of Thermal Sciences 66, 82-90, 2013.
- [4]. RahulTarodiya, J. Sarkar, J. V. Tirkey, “Performance of flat fin tube automotive radiator using Nano fluids as coolants”. National Conference on Emerging Trends in Mechanical Engineering ETME – 2012.
- [5]. Efeovbokhan, Vincent Enontiemonria, Ohiozua, Ohireme Nathaniel, “Comparison of the cooling effects of a locally formulated car radiator coolant with water and a commercial coolant”.
- [6]. S.M. Peyghambarzadeh , S.H. Hashemabadi , S.M. Hoseini , M. SeifiJamnani “Experimental study of heat transfer enhancement using water/ethylene glycol based Nano fluids as a new coolant for car radiators”. International Communications in Heat and Mass Transfer 38, 1283–1290, 2011.
- [7]. S.M. Peyghambarzadeh, S.H. Hashemabadi, M. Naraki, Y. Vermahmoudi," Experimental study of overall heat transfer coefficient in the application of dilute Nano fluids in the car radiator".Applied Thermal Engineering 52, 8-16, 2013.

- [8]. D. Madhesh, R. Parameshwaran, S. Kalaiselvam" Experimental investigation on convective heat transfer and rheological characteristics of Cu–TiO₂ hybrid nanofluids".*Experimental Thermal and Fluid Science* 52, 104–115, 2014.
- [9]. Navid Bozorgan, Komalangan Krishnakumar, Nariman Bozorgan," Numerical Study on Application of CuO/Water Nano fluid in Automotive Diesel Engine Radiator ".*Modern Mechanical Engineering*,130-13, Sep.2012.
- [10]. L. Syam Sundar, Manoj K. Singh, Igor Bidkin, Antonio C.M. Sousa, " Experimental investigations in heat transfer and friction factor of magnetic Ni Nano fluid flowing in a tube". *International Journal of Heat and Mass Transfer* 70, 224–234, 2014.
- [11]. Changhua Lin , Jeffrey Saunders , Simon Watkins, " The Effect of Changes in Ambient and Coolant Radiator Inlet Temperatures and Coolant Flow rate on Specific Dissipation". *SAE Technical Paper Series*, 01- 0579, 2000.
- [12]. Shaolin Maoa, Changrui Cheng, Xianchang Li, Efsthios E. Michaelides, "Thermal/structural analysis of radiators for heavy-duty trucks". *Applied Thermal Engineering* 30 1438-1446, 2010.
- [13]. M.M. Elias, I.M. Mahbubul, R. Saidur, M.R. Sohel, I.M. Shahrul, S.S. Khaleduzzaman, S. Sadeghipour, " Experimental investigation on the thermo-physical properties of Al₂O₃.nanoparticles suspended in car radiator coolant". *International Communications in Heat and Mass Transfer* 54, 48–53, 2014.
- [14]. Adnan M. Hussein, R.A. Bakar, K. Kadirgama, K.V. Sharma, " Heat transfer enhancement using Nano fluids in an automotive cooling system". *International Communications in Heat and Mass Transfer* 53, 195– 202, 2014.
- [15]. Adnan M. Hussein, R.A.Bakar, K.Kadirgama, "Study of forced convection Nano fluid heat transfer in the automotive cooling system". *Case Studies in Thermal Engineering* 50–61, 2014.
- [16]. C. Oliet, A. Oliva, J. Castro, C.D. Perez-Segarra, "Parametric studies on automotive radiators". *Applied Thermal Engineering* 27, 2033–2043, 2007.
- [17]. Rahul A. Bhogare B. S. Kothawale, "A Review on applications and challenges of Nano-fluids as coolant in Automobile Radiator". Lee D. W., Bateman W.J.D, Owens N., 2007, *Efficiency of Oil/Water Separation Controlled by Gas Bubble Size and Fluid Dynamics within the Separation Vessel*, GLR Solutions, Calgary, Canada, 2007.
- [18]. Wilkinson D., Waldie B., Mohamad M. I., Lee H. Y., 1999, Baffle plate configurations to enhance separation in horizontal primary separators. *Short communication. Chemical Engineering Journal*, 77, 221-226
- [19]. Zhang L., Xiao H., Zhang H., Xu L., Optimal design of a novel oil-water separator for raw oil produced from ASP flooding, *Journal of Petroleum Science and Engineering*, 59, 213-218, 2007.
- [20]. ANSYS.ANSYS CFX-Solver Theory Guide, 14th edition, ANSYS Inc., 2015.